9th International Symposium on Hydraulic Structures Roorkee, India 24-27 October 2022
ISBN 978-1-958416-07-5 DOI: https://doi.org/10.26077/11eb-458d

Surface Velocities and Free-surface Aeration in a Converging Smooth Chute during a Major Flood Event

H. Chanson[1] & C.J. Apelt[1]
[1]*The University of Queensland, School of Civil Engineering, Brisbane, Australia*
E-mail: h.chanson@uq.edu.au

Abstract: *In a free-surface spillway, the upstream flow is non-aerated and the flow becomes a strong air-water mix downstream of the onset location of air entrapment. Field observations were conducted over a large dam's spillway during a major flood event. The wastewaterway system was a smooth converging chute with a longitudinal slope of 11.3°: the Chinchilla Minimum Energy Loss weir on the Condamine River (Australia). Detailed quantitative measurements were undertaken in the high-speed chute flows with strong turbulence and high Reynolds numbers at the early part and later part of a major flood event. During this exceptional flood, the spillway passed nearly three times the design discharge capacity at the peak for the event. Down the smooth chute, the observations indicated that the onset of free-surface aeration was a complicated transient three-dimensional process. A robust optical flow (OF) technique was applied and delivered physically-meaningful surface velocities in the air-water flow region. The streamwise surface velocities were reasonably close to backwater calculations. The data presented large streamwise surface velocity fluctuations in the aerated flow region, with* Tu_s *~ 150-200%, on the centreline consistent with self-aerated flow measurements using dual-tip phase detection probe in laboratory. Overall, the study demonstrated the application of optical techniques to prototype smooth spillway flows, as well as some intrinsic difficulties with field investigations.*

Keywords: *Prototype velocity measurements; Smooth converging chute; Self-aeration; Optical techniques; Minimum Energy Loss weir.*

1. Introduction

In most overflow spillways, the upstream flow is non-aerated and a strong air-water mix develops downstream of the onset region of air entrapment (Halbronn et al. 1953, Wood et al. 1983). At the upstream end of an un-controlled spillway, the flow is rapidly accelerated as it changes from a critical motion at the weir crest to a supercritical motion on the chute in a relatively smooth manner (Halbronn 1952, Keller and Rastogi 1975). A turbulent boundary layer develops along the invert from the upstream end (Ippen et al. 1955, Chanson 1997a). On a steep spillway chute, the onset of free-surface aeration is typically observed when the outer edge of the boundary layer starts to interact with the free-surface (Lane 1936, Rao and Rajaratnam 1961). These interactions can be explosive with strong air-water ejections (Chanson 2013, Zabaleta and Bombardelli 2020). On flat chutes, in contrast, the inception region presents a rippled surface with small free-surface instabilities tending to become a choppy water surface once aeration takes place (Michels and Lovely 1953, Chanson 1997b). It was argued that the onset of aeration on flat spillways results from a combination of longitudinal vortices' breakdown and of gravity waves produced by roughness and irregularities at the boundaries (Levi 1965,1967, Anwar 1994). Yet, the two theories are not exclusive as discussed by Toro et al. (2017) and Chanson (2021), based upon three-dimensional CFD computations and detailed prototype observations respectively. The onset processes of free-surface aeration on spillway chutes are illustrated in Figure 1 by high-shutter speed photographs of the inception region in steep (Fig. 1A) and flat (Fig. 1B) prototype chutes.

During the last five decades, a number of overflow embankment designs were developed including earth dam spillway with precast concrete blocks (Pravdivets and Bramley 1989, Chanson 2001), concrete protection of the downstream embankment slope (McLean and Hansen 1993, FEMA 2014) and Minimum Energy Loss weir (McKay 1971). The Minimum Energy Loss (MEL) weir design was developed specifically for the river catchments affected by heavy tropical and sub-tropical rainfalls with very flat gradients, i.e. $S_o \sim 0.1\%$ (McKay 1971, Turnbull and McKay 1974).

In the current contribution, a series of field observations were conducted in a large protype MEL weir during a major flood event in late 2021. The data were analysed, and the results are discussed herein. Detailed quantitative measurements were performed in terms of the surface velocity field in the high-speed, high-Reynolds-number overflow. Some key features of the inception region of free-surface aeration were described, showing the onset of air entrapment being a complicated process, while the air-water flow was characterised by large streamwise surface velocity fluctuations.

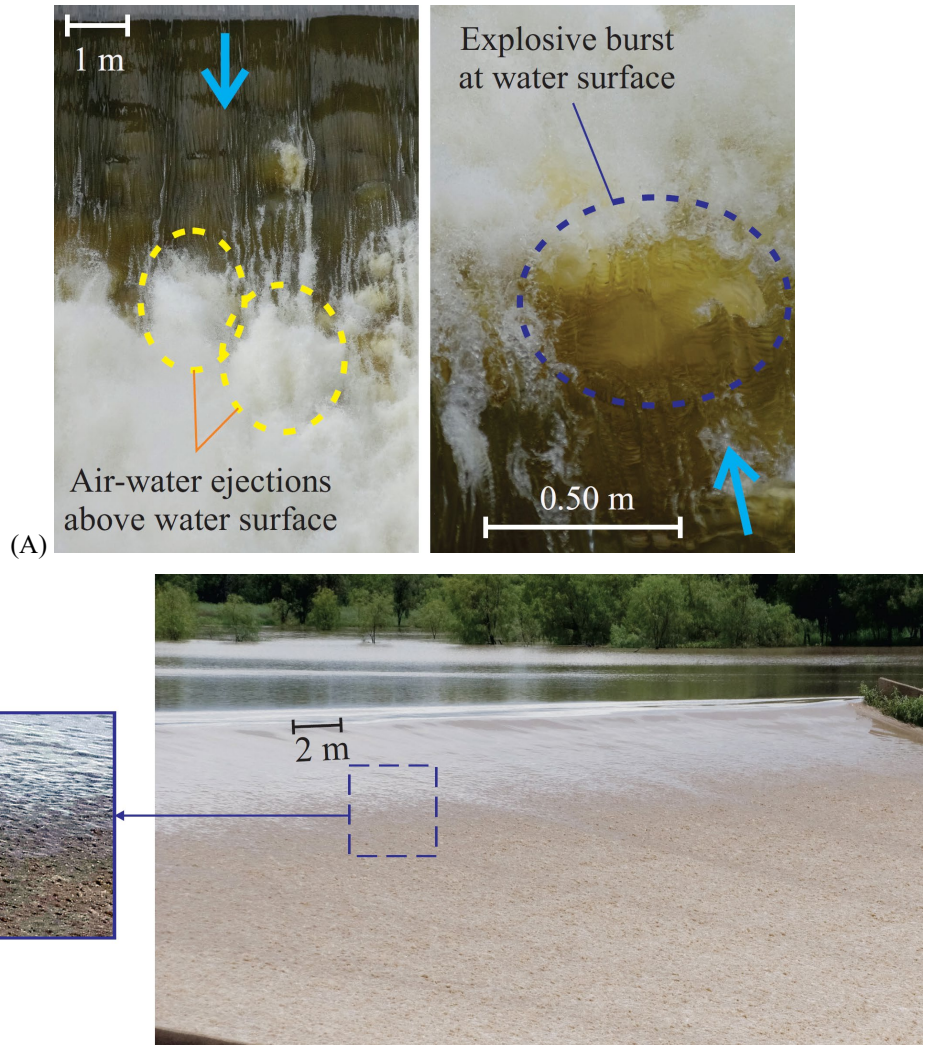

Figure 1. High-shutter speed photographs of the inception region of free-surface aeration on prototype chute spillways. (A) Explosive burst at and air-water ejections above the water surface at Hinze dam (Australia) on 27 March 2021 ($\theta = 37.5°$ [at inception], $Re = 2.34 \times 10^7$, Shutter speed: 1/8,000 s). (B) Rippled/choked water surface at the water surface of the inception region at Chinchilla MEL weir (Australia) on 27 November 2021 ($\theta = 11.3°$, $Re = 2.3 \times 10^6$ [at inception], Shutter speed: 1/8,000 s).

2. Study site and Methodology

2.1. Study site

The Chinchilla MEL weir (QLD, Australia) is located on the Condamine River, on the northern part of the Murray-Darling basin. The weir was completed in 1973 to provide irrigation water, and it is listed as a "large dam" by ICOLD (1984). The catchment area is 19,192 km^2. The structure is a 14 m high earthfill embankment with a 410 m long dam crest (incl. abutments) and equipped with an overflow spillway (Figs. 2A & 2B) (Turnbull and McKay 1974). The design spillway capacity is 850 m^3/s corresponding to bank full. The spillway consists of a broad crest, 3.05 m long, and 213.4 m wide, followed by a 60.6 m long smooth converging chute with a 11.3° slope (1V:5H) and no dissipation structure was built. The downstream width of the chute is 81.2 m and the chute convergence is $\partial B/\partial x = -2.18$. The overflow section is concrete-lined, with a series of drains to reduce seepage pressure. The Chinchilla weir was designed to pass the design discharge (Q_{des} = 850 m^3/s, bank full) with an afflux of less than 1.83 m. Between 1973 and 2022, the weir was overtopped by a number of large flood events, including a number of overflows larger than the design flow. The weir operated safely and properly, and inspections after the flood showed no damage.

Figure 2. Chinchilla Minimum Energy Loss (MEL) weir (QLD, Australia). (A) Overflow on 27 November 2021 (Q = 121 m^3/s); (B) Hydraulic jump at the chute toe on 27 November 2021 (Q = 121 m^3/s, Shutter speed: 1/2,500 s); (C) Camera tripod setup on the lower right bank; (D) High-water marks on the right bank on 15 December 2021

2.2. Instrumentation

The water discharge was deduced from the measured reservoir elevation, using the predicted discharge coefficient, based upon the drawings as constructed (Irrigation and Water Supply Commission 1972).

Visual, photographic and cinematographic records were undertaken from the right bank of the spillway and from the right river bank downstream of the spillway toe. Figure 2 present hand-held photographs taken from several locations. The observations were conducted using three dSLR Pentax™ cameras with sensor resolutions between 12 Mpx and 24 Mpx, a digital camera Sony™ RC100VA and an iPhone XI. The dSLR cameras were equipped with full-frame prime lenses producing photographs and movies with negligible barrel distortion. The dSLR camera movies were recorded in high definition (1920×1080 px) at 30 fps and 60 fps.

The analyses of surface features were conducted using both high-shutter speed photographs and video movies. For all the cases, the tracking and measurements of the water surface features were conducted manually to guarantee the best quality control, owing to the complexity of the prototype flow's turbulent motion, characterised by very rapid and unpredictable changes with time and space. Further, a number of movies were taken from downstream and analysed using an optical flow (OF) technique, with the camera fixed on a sturdy professional-grade tripod (Fig. 2C). The Optical Flow (OF) is a set of tools, detecting the flow motion between consecutive frames based upon brightness intensity gradients (Bung and Valero 2017, Zhang and Chanson 2018). In the current study, Farnebäck's (2003) OF technique was applied to calculate the surface velocity field. The Farneback OF technique was applied with OF parameters previously validated in laboratory for surface velocity field (Arosquipa Nina et al. 2022) and used for the Hinze Dam prototype spillway data sets (Chanson 2022). It is acknowledged that the OF calculations were not truly 'calibrated' owing to the significant number of intrinsic difficulties with field observations during flood events, including un-controlled optical conditions (Chanson 2021). Since the camera field of view was perpendicular to the spillway chute, the raw data included the vertical and horizontal transverse surface velocity components recorded at various vertical elevations. The streamwise surface velocity was deduced from the vertical surface velocity component and invert slope based upon geometric considerations, assuming a two-dimensional flow.

2.3. Flow conditions

From mid-November 2021, some solid rain fell in the Condamine River catchment area upstream of Chinchilla. Some widespread major flooding was reported in the upstream catchment. The Chinchilla weir overflowed for more than one month, with the peak headwater observed on 5 December 2021 morning. Observations of overflow discharges are presented in Figure 3. For seven days, the spillway discharged a flow rate greater than the design discharge, with a peak flow about 1,930 m^3/s corresponding to 2.3 times the design discharge. Note that the inspection on 15 December 2021 confirmed that the abutments were overtopped by nearly 3 m of water at the peak of the flood, without damage (Fig. 2D)

The Chinchilla weir overflow was documented on 27 November 2021 and 15 December 2021 (Table 1). The first data set was obtained at the start of the flood event, while the second took place after the peak of the flood (Fig. 3). The flow conditions at the time of observations are detailed in Table 1. Note that the weir overflow could not be witnessed at the peak of the flood, because the access road become submerged when the tailwater elevation exceeds about 290-291 m AHD. The afflux, difference between recorded HWRL and TWRL, was 3.25 m at the peak of the flood event.

Table 1. Overflow observations at Chinchilla Minimum Energy Loss weir (QLD, Australia) during the major flood with its peak on 5 December 2021

Date	Time	Headwater (m AHD)	Tailwater (m AHD)	Q (m^3/s)	Re (at spillway crest)
27 November 2021	12:45-13:20	296.23	287.20	121	2.3×10^6
15 December 2021	12:30-13:30	296.29	287.52	144	2.7×10^6

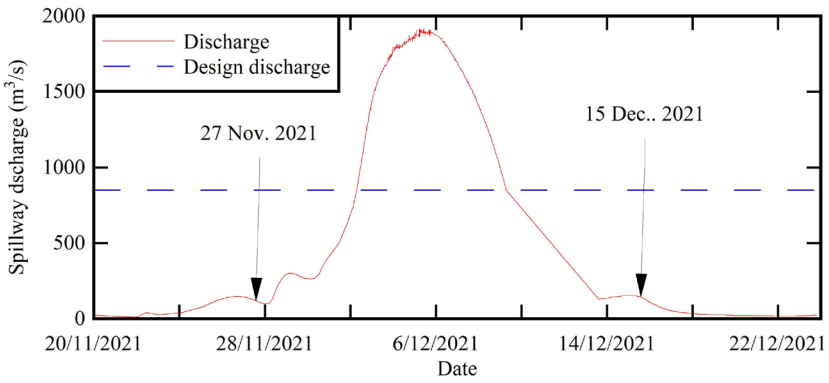

Figure 3. Spillway discharge at Chinchilla Minimum Energy Loss weir (QLD, Australia) during the major flood with its peak on 5 December 2021. Overflow discharge over the spillway chute, excluding the abutment overflows.

3. Basic observations

On both occasions (Table 1), the approach flow was very smooth, and this was confirmed by aerial footages on 21 December 2018 and 3 December 2021. The reservoir flow converged smoothly towards the weir crest and the water surface was waveless and almost still. On both 27 November and 15 December 2021, the flow was critical at the spillway crest which acted as a broad-crested weir, with a ratio of crest length to upstream head over crest of 6.2 and 5.54 respectively. The smooth change on water surface elevation between the upstream reservoir and spillway crest was nicely documented with photographs (Fig. 4A). Immediately downstream of the broad-crest, the water surface was smooth and glassy (Figs. 2A, 2B & 4A). On 27 November 2021, a few logs were trapped at the crest, and their wake was clearly seen at the surface of the non-aerated flow. Further downstream, the wake progressively disappeared in the self-aerated air-water flow region (Fig. 4B).

As the flow accelerated down the smooth converging chute, the glassy free-surface become rough and choppy, before becoming self-aerated, i.e. the inception region. The inception region showed a progressive transition of the surface roughness, from a smooth glassy surface, to a rough, coarse-sand-paper-like appearance and later to a very-rough choppy surface (Fig. 4). The self-aerated region presented a beige colour, evidence of a three-phase air-water sediment motion. Such an observation was well-documented visually on both 27 November and 15 December 2021, as well as during an earlier overflow on 8 November 1997 (Toombes and Chanson 2007).

The location x_I of the inception region of self-aeration was recorded during both overflows, and the data are reported in Table 2 (column 5). The corresponding water depth d_I was deduced for the backwater calculations (Table 2, column 6). The observations are compared to the correlations of Cain and Wood (1981) for a smooth prismatic channel, assuming k_s = 1 mm as for the backwater calculations (see below). The comparative results (Table 2) showed a close agreement in terms of the water depth at inception, while the observed location data presented more scatter, possibly caused by the wide spread of the inception region, while the flow convergence was expected to induce a slower growth in bottom boundary layer compared to prismatic chutes.

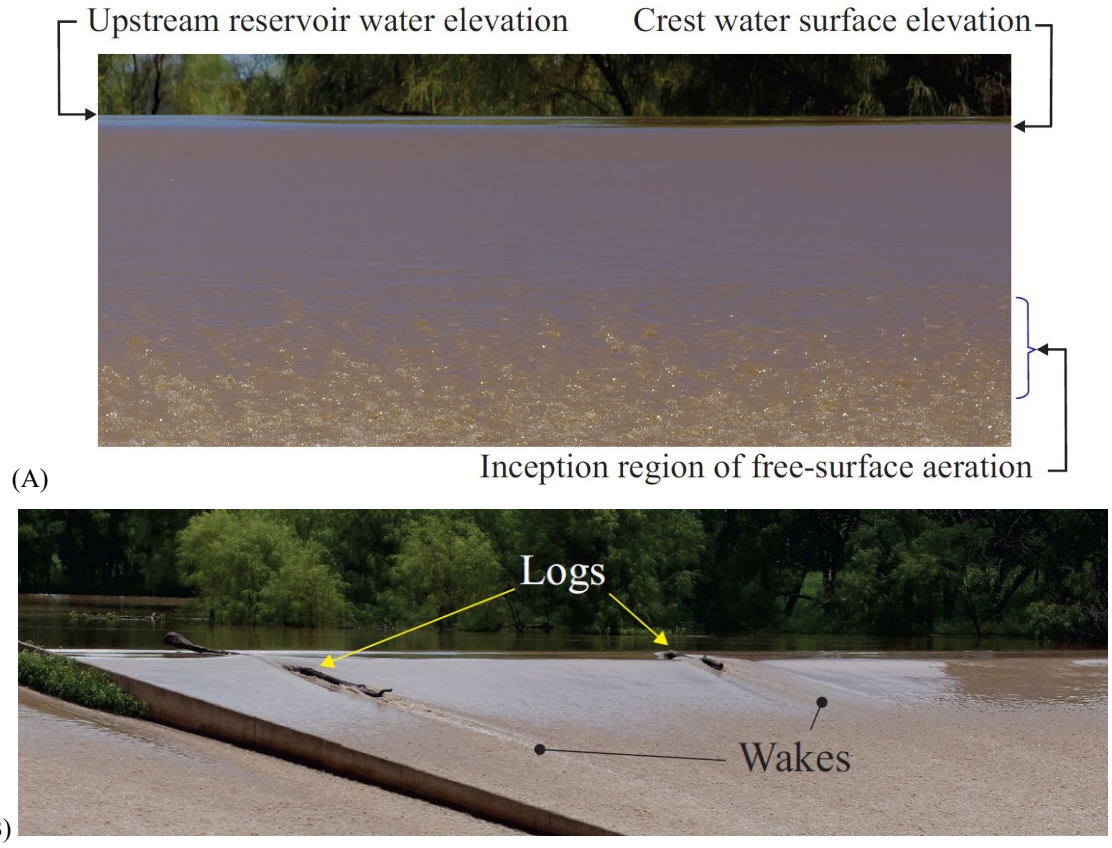

Figure 4. Photographic observations of the spillway operation at Chinchilla Minimum Energy Loss weir (QLD, Australia) during the major flood with its peak on 5 December 2021. (A) Upstream flow viewed from downstream on 15 December 2021; (B) Timber logs blocked at the spillway crest on 27 November 2021.

Table 2. Location and water depth at the inception of free-surface aeration at Chinchilla Minimum Energy Loss weir (QLD, Australia) during the major flood with its peak on 5 December 2021

Date	Time	Q (m^3/s)	Head above crest (m)	x_I ([1]) (m)	d_I ([2]) (m)	x_I predicted ([3]) (m)	d_I predicted ([3]) (m)
27 November 2021	12:45-13:20	121	0.49	7.5	0.11	10.2	0.10
15 December 2021	12:30-13:30	144	0.55	13.4	0.12	11.6	0.12

Notes: ([1]) statistical median of photographic and movie data; ([2]) water depth estimate deduced from present backwater calculation; ([3]) Correlations of Cain and Wood (1981).

At the toe of the spillway chute, the high-velocity self-aerated flow impinged into the tailwater and a hydraulic jump formed (Fig. 2C). The jump was stationary and very stable, located on the underwater sloping chute on both days. The position of the jump was controlled by the tailwater conditions and the very-flat Condamine River channel bed slope downstream of Chinchilla. The jump roller was highly turbulent and fluctuating about its mean position. Both visual and video movie observations indicated strong three-dimensional large-scale vortices in the roller. The interactions of these large turbulent structures with the roller free-surface created large scars and surface features, with length-scales comparable to the roller height.

4. Surface velocity measurements

Based upon the video movies taken from downstream, the Optical Flow (OF) data encompassed the surface velocity, measured in the plane parallel to the invert. Both the longitudinal velocity component V_s and the transverse surface velocity component V_t were extracted on the left chute centreline. In the current study, the data provided meaningless results in the non-aerated flow region. This was most likely caused by the shiny surface glare, seen in Figures 2 and 4, upstream of the inception region. Meaningful OF results were achieved in the self-aerated flow region (see below). The finding differed from the OF observations at the Hinze Dam spillway (Chanson 2021,2022).

For the left chute, the centreline OF surface velocities were compared to the ideal fluid flow theory and to the backwater equation. On an uncontrolled chute spillway, the flow is accelerated by the gravity force component in the flow direction, and the ideal velocity V_{max} at a sampling location on the chute is derived from the Bernoulli principle:

$$V_{max} = \sqrt{2 \times g \times (H_1 - d \times \cos\theta)} \quad (1)$$

where H_1 is the upstream total head above the sampling point, θ is the channel slope and d is the water depth (Chanson 2004). For a non-uniform and steady real fluid flow, the backwater calculations are based upon the differential form of the energy equation and performed assuming that the flow is gradually varied. For a rectangular channel of non-constant width and slope, the backwater equation yields (Chanson 2004, pp. 377-381):

$$\frac{\partial d}{\partial x} \times (\cos\theta - Fr^2) = -\frac{\partial z_o}{\partial x} - S_f + d \times \sin\theta \times \frac{\partial \theta}{\partial x} + Fr^2 \times \frac{d}{B} \times \frac{\partial B}{\partial x} \quad (2)$$

$$Fr = \frac{Q}{\sqrt{g \times d^3 \times B}} \quad (3)$$

With d the water depth, S_f the friction slope, θ the invert slope and B the free-surface width. At Chinchilla weir, the channel is rectangular, with constant slope and a reducing width. Thus, the backwater equation becomes:

$$\frac{\partial d}{\partial x} \times (\cos\theta - Fr^2) = -\frac{\partial z_o}{\partial x} - S_f + Fr^2 \times \frac{d}{B} \times \frac{\partial B}{\partial x} \quad (4)$$

with $\cos\theta = 0.9806$, $\sin\theta = 0.196$, and $\partial B/\partial x = -2.1805$ at the Chinchilla MEL weir.

The results showed a relatively close agreement between the streamwise OF surface velocity and the backwater-calculated velocity downstream of the onset region, both qualitatively and quantitatively (Fig. 5). Figure 5 presents a typical comparison in terms of streamwise surface velocity component V_s, with data for one movie. The ideal fluid flow estimates are shown with a solid green curve and the backwater calculations are the dashed red curve. In Figure 5B, the streamwise surface velocity standard deviation v_s' and transverse surface velocity standard deviation v_t' are added for completeness. In Figure 5, the data were collected on the centreline of the field of view and the vertical axis is the vertical elevation in m AHD.

First, the OF streamwise surface velocity increased with decreasing vertical elevation (Fig. 5). Second the OF data showed some poor outcome in the non-aerated developing flow region. For $z_o > 294$ m AHD, the poor OF results were caused by the surface glare seen in Figures 2A and 4. Third, the surface velocity data agreed relatively well with the backwater calculations developed for the converging chute (see above). For $z_o < 288$ m AHD, a lack of match with backwater estimate might be caused by optical artifacts above the hydraulic jump roller, caused by spray and splashing seen in Figure 2B. Fourth, the OF data output quality was closely linked to the quality of the original movies. This encompassed the camera position ideally placed perpendicularly to the spillway chute, and the camera body and lens equipment, with all the present data set acquired with professional-grade full-frame prime lenses, following earlier studies (Arosquipa Nina et al. 2022, Chanson 2021,2022). Furthermore, the movie definition delivered improved outputs with higher spatial resolutions, i.e. less millimetres per pixel. It is worth to mention that both field data sets were filmed under good weather conditions, hence decent lighting conditions.

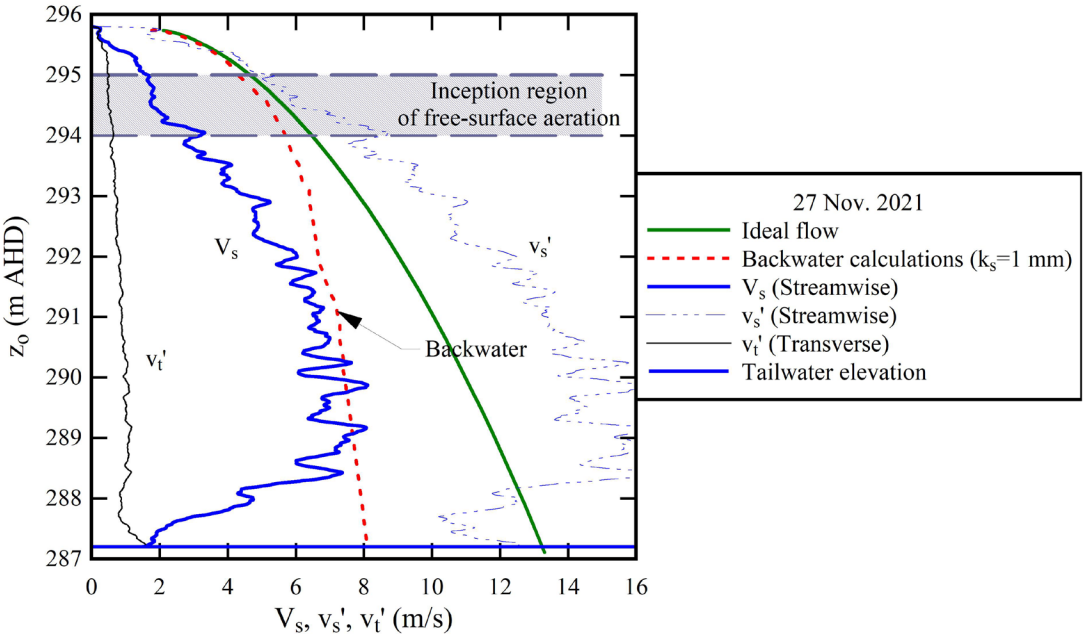

Figure 5. OF surface velocity data at Chinchilla Minimum Energy Loss weir (QLD, Australia) during the major flood with its peak on 5 December 2021. Comparison with ideal fluid flow velocity and backwater calculations. Analyses of image centreline. Streamwise surface velocity and standard deviations of streamwise and transverse velocity components on 27 November 2021, Camera: Pentax K-3 with Pentax FA*300mm f4.5 lens & HD TC 1.4x, HD movie (1,920×1080 px), 30 fps, Number of analysed frames:840, Spatial resolution: 5.15mm/px, Reference 1136.

The OF surface velocity characteristics were analysed in the self-aerated flow region, in terms of the standard deviations of the streamwise and transverse surface velocity. The weighted averages are presented in Table 3, together with the number of analysed frames, the frame rate and the spatial resolutions. The large number of analysed frames must be noted in the current study (Table 3, 4th column). The streamwise velocity data presented large surface turbulent intensity $Tu_s = v_s'/V_s \sim 1.7$-2 (Table 3). Such large values were likely caused by a combination of relatively large velocity fluctuations initiated by surface wave motion and of true turbulence. The data were quantitatively of the same magnitude as the field measurements in the Hinze Dam spillway (Chanson 2022) and as laboratory self-aerated flow data (Chanson and Toombes 2002, Arosquipa Nina et al. 2022). In the other hand, the transverse velocity data exhibited much lower transverse surface turbulent intensity $Tu_t = v_t'/V_s \sim 0.11$-0.17, likely induced by the smooth

convergence of the flow. The ratio v_t'/v_s' was between 0.06 and 0.1 (Table 3), implying a strong anisotropy of the surface turbulence. The observations were close to reported values of v_t'/v_s' in rough turbulent boundary layers (Schlichting and Gersten 2000) and on the Hinze Dam prototype spillway (Chanson 2022).

Table 3. OF surface turbulence characteristics of self-aerated flow at Chinchilla Minimum Energy Loss weir (QLD, Australia) during the major flood with its peak on 5 December 2021

Date	Q (m^3/s)	Frame rate (fps)	Total Nb of analysed frames	Spatial resolution (mm/px)	v_s'/V_s (1) (2) (3)	v_t'/V_s (1) (2) (3)	v_t'/v_s' (1) (2) (3)
27 November 2021	121	30 & 60	6,660	5.15 & 7.2	1.71	0.111	0.064
15 December 2021	144	30 & 60	92,310	5.8 & 8.3	2.09	0.165	0.096

Notes: V_s: time-averaged streamwise surface velocity; v_s': standard deviation of streamwise surface velocity; v_t': standard deviation of transverse surface velocity; (1) weighted average for all analysed movies; (2) analyses of image centreline; (3) observations for $288 < z_o < 293$ m AHD.

5. Conclusion

The Chinchilla weir in Queensland, Australia is a large dam equipped with an unusual overflow spillway system, i.e. a minimum energy loss (MEL) design. The approach flow is very smooth and streamlined before it reaches the broad-crest, and then continues down a converging smooth chute. In the current study, the spillway chute was observed and documented during two days, at the start and towards the end of a major flood event peaking on 5 December 2021.

The field observations showed the smooth streamlining of the reservoir waters into the spillway crest and chute. Downstream of the crest, the chute flow presented a very smooth and glassy free-surface. On 17 November 2021, the presence of large logs, blocked on the crest, had no major impact on the chute flow. Further downstream, the water surface became rough and choppy, immediately before the flow became self-aerated. The inception region presented a gradual variation of the surface roughness, from a smooth glassy surface, to a coarse-sand-paper-like appearance and then a very-rough choppy surface. Both the upstream non-aerated and self-aerated flow regions exhibited a brown colour indicating a large amount of suspended sediments.

An optical flow (OF) technique was applied to relatively long-duration movies recorded from a sturdy tripod facing the left section of the spillway chute. The time-averaged streamwise surface velocities were successfully compared to the application of the backwater calculations for a smooth converging chute, in the self-aerated flow region. The streamwise velocities were about 8-9 m/s at the chute toe. In contrast, the OF data were physically-meaningless in the developing flow region because of optical artifacts. The OF data presented large streamwise surface velocity fluctuations in the aerated flow region, with $Tu_s \sim 150$-200%, consistent with the broad literature on self-aerated flow measurements using dual-tip phase detection probe in laboratory. The ratio of transverse to streamwise surface turbulence intensity v_t'/v_s' was between 0.06 and 0.1, indicating a strong anisotropy of the free-surface turbulence.

6. Acknowledmennts

Hubert Chanson thanks Mr André Chanson and Ms Ya-Hui Chou for their assistance with the field works. He acknowledges Sunwater for providing technical details of the Chinchilla weir spillway, and Leigh Cook and Tobias Burwood (Western Downs Regional Council) for providing photographic information on the flood event. He also thanks Mr Barton Maher (QLD Department of Regional Development, Manufacturing and Water), Jeff Dann (Sunwater), Mr Rui (Ray) Shi (The University of Queensland), Dr Carlos Gonzalez (QLD Department of Transport and Main Road) for their assistance and advice.

In line with recommendations of the International Committee on Publication Ethics (COPE) and the Office of the Commonwealth Ombudsman (Australia), Hubert Chanson declares a major conflict of interest with Matthias Kramer (UNSW, Canberra).

7. References

Anwar, H.O. (1994). "Self-Aerated Flows on Chutes and Spillways - Discussion." *Journal of Hydraulic Engineering*, ASCE, Vol. 120, No. 6, pp. 778-779.

Arosquipa Nina, Y, Shi, R., Wűthrich, D., and Chanson, H. (2022). "Intrusive and Non-Intrusive Two-Phase Air-Water Measurements on Stepped Spillways: a Physical Study." *Experimental Thermal and Fluid Science*, Vol. 131, Paper 110545, 22 pages, 4 movies and a digital appendix (6 pages) (DOI: 10.1016/j.expthermflusci.2021.110545).

Bung, D.B., and Valero, D. (2016). "Optical Flow Estimation in Aerated Flows." *Journal of Hydraulic Research*, IAHR, Vol. 54, No. 5, pp. 575-580 (DOI: 10.1080/00221686.2016.1173600).

Cain, P., and Wood, I.R. (1981). "Measurements of Self-aerated Flow on a Spillway." *Journal Hydraulic Division*, ASCE, 107, HY11, pp. 1425-1444.

Chanson, H. (1997). "Air Bubble Entrainment in Open Channels. Flow Structure and Bubble Size Distributions." *International Journal of Multiphase Flow*, Vol. 23, No. 1, pp. 193-203 (DOI: 10.1016/S0301-9322(96)00063-8).

Chanson, H. (1997b). "Air Bubble Entrainment in Free-Surface Turbulent Shear Flows." *Academic Press*, London, UK, 401 pages.

Chanson, H. (2001). "The Hydraulics of Stepped Chutes and Spillways." *Balkema*, Lisse, The Netherlands.

Chanson, H. (2004). "The Hydraulics of Open Channel Flow: An Introduction." *Butterworth-Heinemann*, 2nd edition, Oxford, UK, 630 pages.

Chanson, H. (2013). "Interactions between a Developing Boundary Layer and the Free-Surface on a Stepped Spillway: Hinze Dam Spillway Operation in January 2013." *Proc. 8th International Conference on Multiphase Flow ICMF 2013*, Jeju, Korea, 26-31 May, Gallery Session ICMF2013-005 (Video duration: 2:15). {https://www.youtube.com/watch?v=cKHDrkNFfC0&t=3s}

Chanson, H. (2021). "Stepped Spillway Prototype Operation, Spillway Flow and Air Entrainment: the Hinze Dam, Australia." *Hydraulic Model Report No. CH123/21*, School of Civil Engineering, The University of Queensland, Brisbane, Australia, 183 pages (DOI: 10.14264/c8d5280).

Chanson, H. (2022). "On Air Entrapment Onset and Surface Velocity in High-Speed Turbulent Prototype Flows." *Flow Measurement and Instrumentation*, Vol. 83, Paper 102122, 9 pages (DOI: 10.1016/j.flowmeasinst.2022.102122).

Chanson, H., and Toombes, L. (2002). "Air-Water Flows down Stepped chutes: Turbulence and Flow Structure Observations." *International Journal of Multiphase Flow*, Vol. 28, No. 11, pp. 1737-1761 (DOI: 10.1016/S0301-9322(02)00089-7).

Farnebäck, G. (2003). "Two-frame motion estimation based on polynomial expansion." *Proc. Scandinavian conference on Image analysis*, Springer, Berlin, Heidelberg, pp. 363-370.

FEMA (2014). "Overtopping protection for dams." *Technical Manual P-1015*, US Bureau of Reclamation, 462 pages.

Halbronn, G. (1952). "Etude de la Mise en Régime des Ecoulements sur les Ouvrages à Forte Pente. Applications au Problème de l'Entraînement d'Air." *Journal La Houille Blanche*, No. 1, pp. 21-40; No. 3, pp. 347-371; No. 5, pp. 702-722 (in French).

Halbronn, G., Durand, R., and Cohen de Lara, G. (1953). "Air Entrainment in Steeply Sloping Flumes." *Proc. 5th IAHR Congress*, IAHR-ASCE, Minneapolis, USA, pp. 455-466.

ICOLD (1984). "World Register of Dams - Registre Mondial des barrages - ICOLD." *International Commission on Large Dams*, Paris, France, 753 pages.

Ippen, A.T., Tankin, R.S., and Raichekn, F. (1955). "Turbulence measurements in free- surface flow with an impact tube-pressure transducer combination." Technical Report No. 20, MIT, Department of Civil and Sanitary Engineering, 112 pages.

Irrigation and Water Supply Commission (1972). "Chinchilla weir layout. As constructed." *Drawing L44375 75313*, Version B, 16/5/1972.

Keller, R.J., and Rastogi, A.K. (1975). "Prediction of Flow Development on Spillways." *Journal of Hydraulic Division*, ASCE, Vol. 101, No. HY9, pp. 1171-1184.

Lane, E.W. (1936). "Recent Studies on Flow Conditions in Steep Chutes." *Engineering News-Record*, Jan. 2, pp. 5-7.

Levi, E. (1965). "Longitudinal Streaking in Liquid Currents." *Journal of Hydraulic Research*, IAHR, Vol. 3, No. 2, pp. 25-39.

Levi, E. (1967). "Macroturbulence Produced by Vortex Breakdown in High Velocity Flows." *Proc. 12th IAHR Congress, Colorado*, USA, Vol. 2, Paper B7, pp. 54-60.

McKay, G.R. (1971). "Design of Minimum Energy Culverts." *Research Report*, Dept of Civil Eng., University of Queensland, Brisbane, Australia, 29 pages & 7 plates.

McLean, F.G., and Hansen, K.D. (1993). "Roller Compacted Concrete for Embankment Overtopping Protection." *Proc. Spec. Conf. on Geotechnical Practice in Dam Rehabilitation*, ASCE, Raleigh NC, USA, L.R. Anderson editor, pp. 188-209.

Michels, V., and Lovely, M. (1953). "Some Prototype Observations of Air Entrained Flow." *Proc. 5th IAHR Congress*, IAHR-ASCE, Minneapolis, USA, pp. 403-414.

Pravdivets, Y.P., and Bramley, M.E. (1989). "Stepped Protection Blocks for Dam Spillways." *International Water Power and Dam Construction*, Vol. 41, No. 7, July, pp. 49-56.

Rao, N.S. Govinda, and Rajaratnam, N. (1961). "On the Inception of Air Entrainment in Open Channel Flows." *Proc. 9th IAHR Congress*, Dubrovnick, Yugoslavia, pp. 9-12.

Schlichting, H., and Gersten, K. (2000). "Boundary Layer Theory." *Springer Verlag*, Berlin, Germany, 8th edition., 707 pages.

Toombes, L., and Chanson, H. (2007). "Surface Waves and Roughness in Self-Aerated Supercritical Flow." *Environmental Fluid Mechanics*, Vol. 7, No. 3, pp. 259-270 (DOI 10.1007/s10652-007-9022-y).

Toro, J.P., Bombardelli, F.A., and Paik, J. (2017). "Detached Eddy Simulation of the Nonaerated Skimming Flow over a Stepped Spillway." *Journal of Hydraulic Engineering*, ASCE, Vol. 143, No. 9, Paper 04017032, 14 pages.

Turnbull, J.D., and McKay, G.R. (1974). "The Design and Construction of Chinchilla Weir - Condamine River Queensland." *Proc. 5th Australasian Conf. on Hydraulics and Fluid Mechanics*, Christchurch, New Zealand, Vol. II, pp. 1-8.

Wood, I.R., Ackers, P., and Loveless, J. (1983). "General Method for Critical Point on Spillways." *Journal of Hydraulic Engineering*, ASCE, Vol. 109, No. 2, pp. 308-312.

Zabaleta, F., and Bombardelli, F.A. (2020). "Eddy-resolving Simulation of Flows over Macroroughness." *Proceedings of RiverFlow2020*, CRC Press, Uijttewaal et al. Editors, pp. 1293-1299.

Zhang, G., and Chanson, H. (2018). "Application of Local Optical Flow Methods to High-Velocity Free-surface Flows: Validation and Application to Stepped Chutes." *Experimental Thermal and Fluid Science*, Vol. 90, pp. 186-199 (DOI: 10.1016/j.expthermflusci.2017.09.010)

Surface Velocities and Free-Surface Aeration in a Converging Smooth Chute During a Major Flood Event

H. Chanson
The University of Queensland, h.chanson@uq.edu.au

C. J. Apelt
The University of Queensland